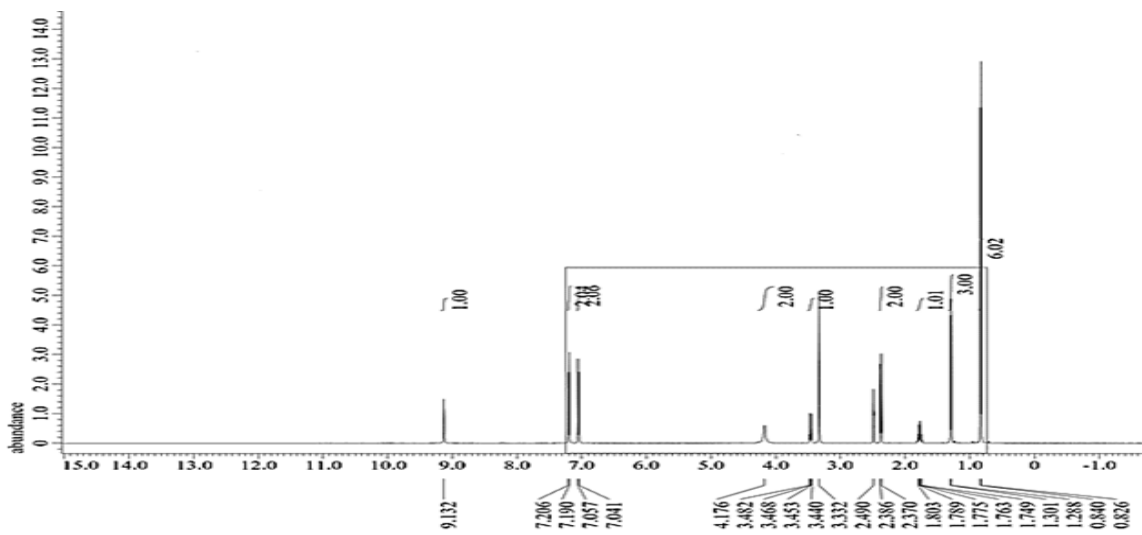


# A Novel Ibuprofen Derivative and Its Complexes: Physicochemical Characterization, DFT Modeling, Docking, In Vitro Anti-Inflammatory Studies, and DNA Interaction

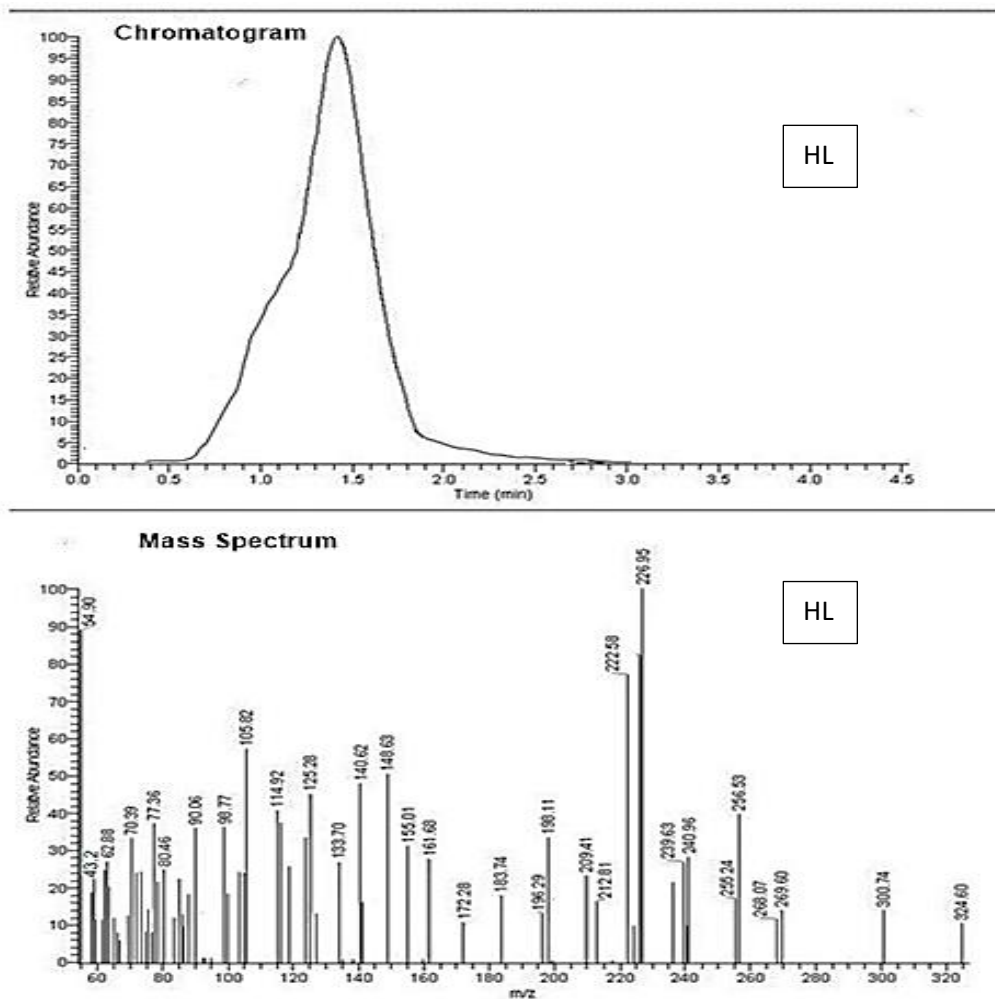
Abbas M. Abbas <sup>1,\*</sup>, Ahmed Aboelmagd <sup>1</sup>, Safaa M. Kishk <sup>2</sup>, Hossam H. Nasrallah <sup>1,3</sup>, Warren Christopher Boyd <sup>4</sup>, Haitham Kalil <sup>1,4,\*</sup> and Adel S. Orabi <sup>1,\*</sup>

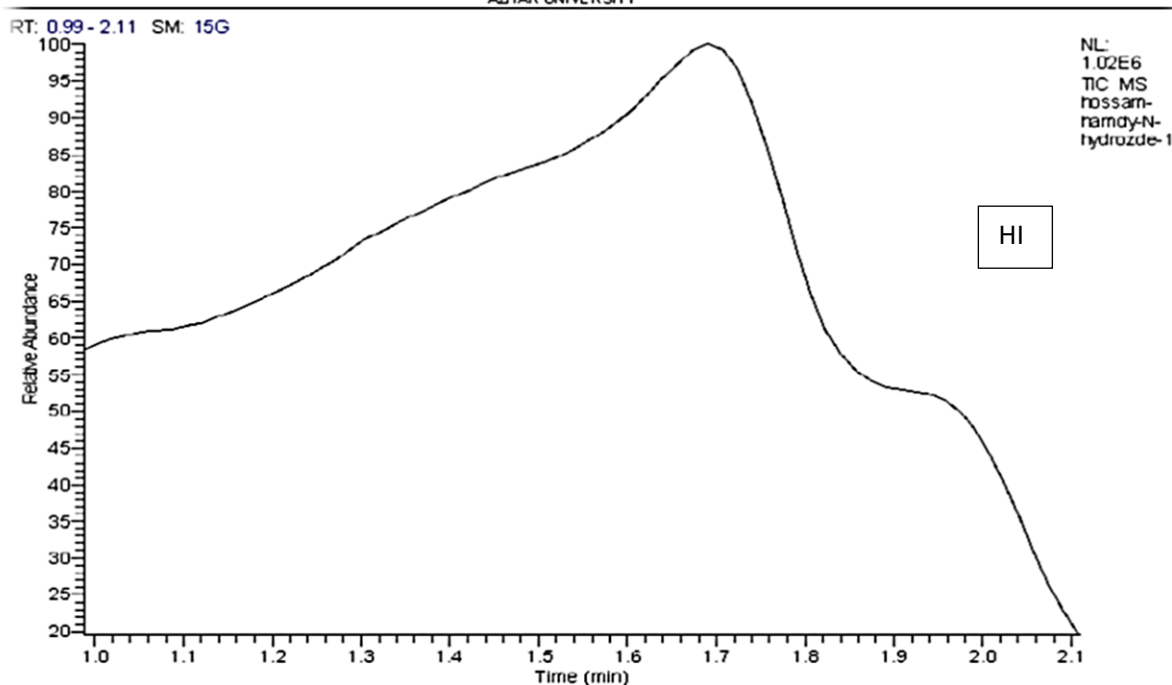
**Table S1:** The <sup>1</sup>H NMR data of the HI and HL.

Comp.	$\delta$ (ppm)
	9.13(1H, br, NH), 7.21-7.04 (4H, m, ArH), 4.18(2H, s, NH <sub>2</sub> ), 3.45(2H, s, CH <sub>2</sub> ), 2.39 (2H, s, CH <sub>2</sub> ), 1.80(1H, s, CH), 1.29 (3H, m, CH <sub>3</sub> ), 0.84-0.82(6H, m, (CH <sub>3</sub> ) <sub>2</sub> ).
HI	<div style="display: flex; justify-content: space-around;"> <div style="text-align: center;"> <p><math>\Delta</math> (ppm) map (experimental)</p> </div> <div style="text-align: center;"> <p><math>\delta</math> (ppm) map (computed)</p> </div> </div>
	11.12(1H, s, OH), 10.03(1H, br, NH), 8.39(1H, s, CH), 7.27-6.63(8H, m, ArH), 3.69(2H, s, CH <sub>2</sub> ), 2.41(2H, s, CH <sub>2</sub> ), 1.83(H, s, CH), 1.39(3H, m, CH <sub>3</sub> ), 0.87-0.82(6H, m, (CH <sub>3</sub> ) <sub>2</sub> ).
HL	<div style="display: flex; justify-content: space-around;"> <div style="text-align: center;"> <p><math>\Delta</math> (ppm) map (experimental)</p> </div> <div style="text-align: center;"> <p><math>\delta</math> (ppm) map (computed)</p> </div> </div>



**Figure S1:** <sup>1</sup>H NMR spectrum of Hydrazide Ibuprofen (HI).





hossam-hamdy-N-hydrozide-1 #93 RT: 1.57 AV: 1 SB: 2 2.71, 2.71 NL: 7.10E4  
T: (0,0) + c EI Full ms [40.00-1000.00]

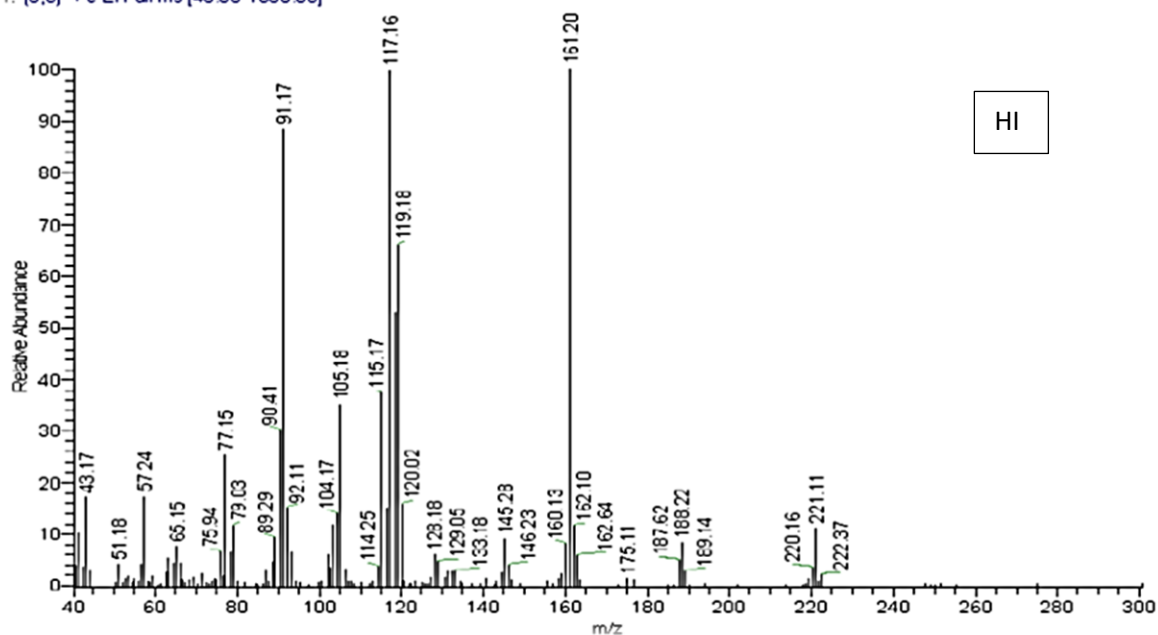
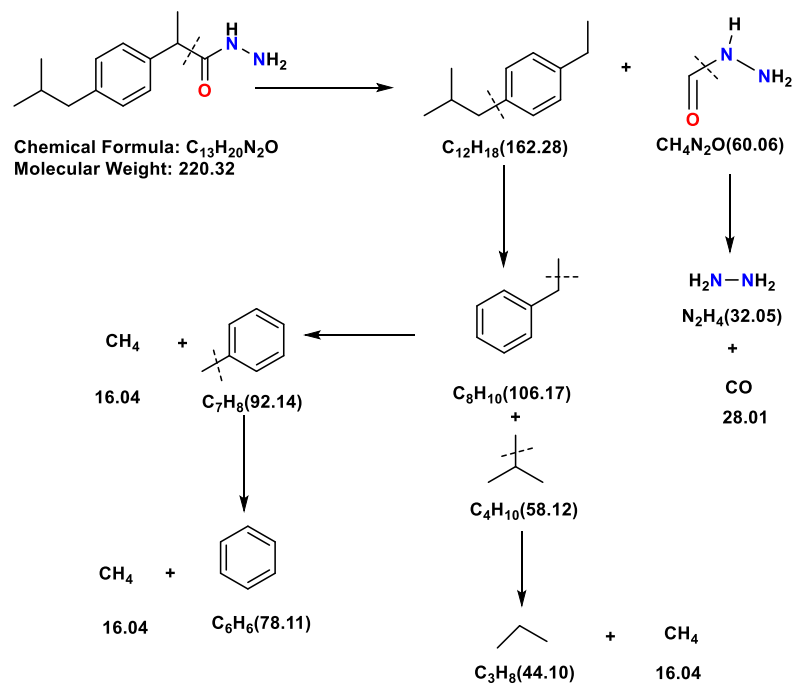
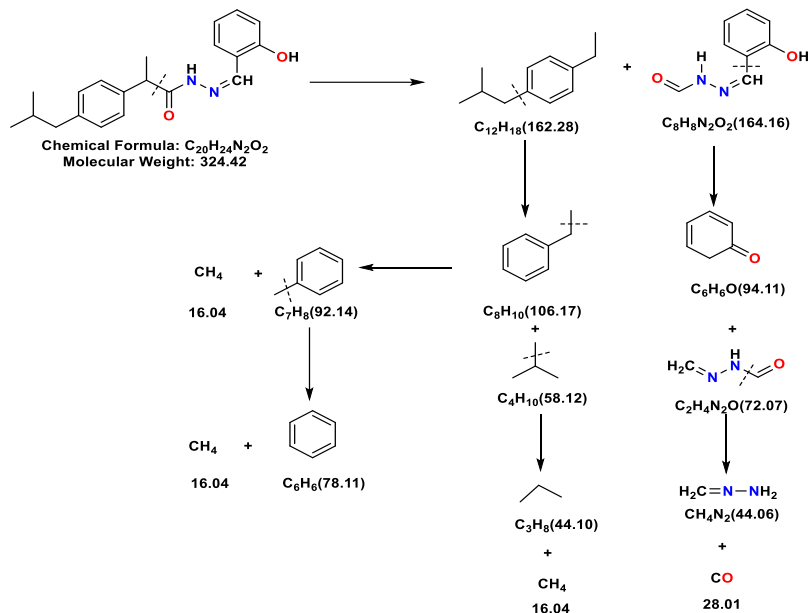


**Figure S2:** Chromatogram and mass spectrum of the Ibuprofen hydrazone (**HL**) and hydrazide (**HI**).



**Scheme S1:** The chromatogram of pathway fragmentation of Hydrazide Ibuprofen (**III**).



**Scheme S2:** The chromatogram of pathway fragmentation of **HL** ligand.

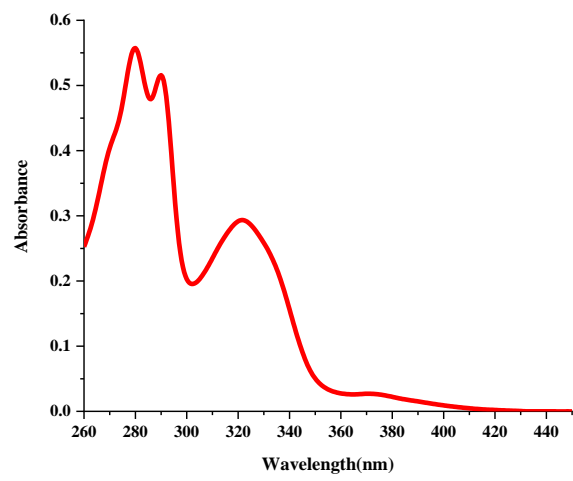


**Figure S3:** UV-Vis. Spectrum of the ligand **HL**.

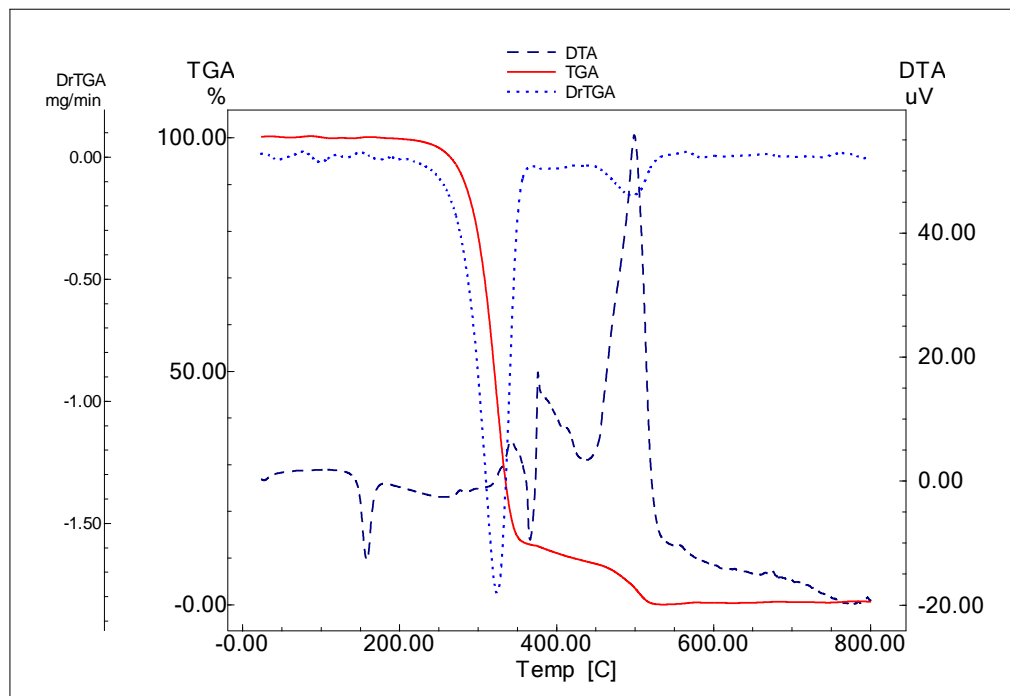


**Figure S4:** Thermal decomposition of Schiff base **HL**.

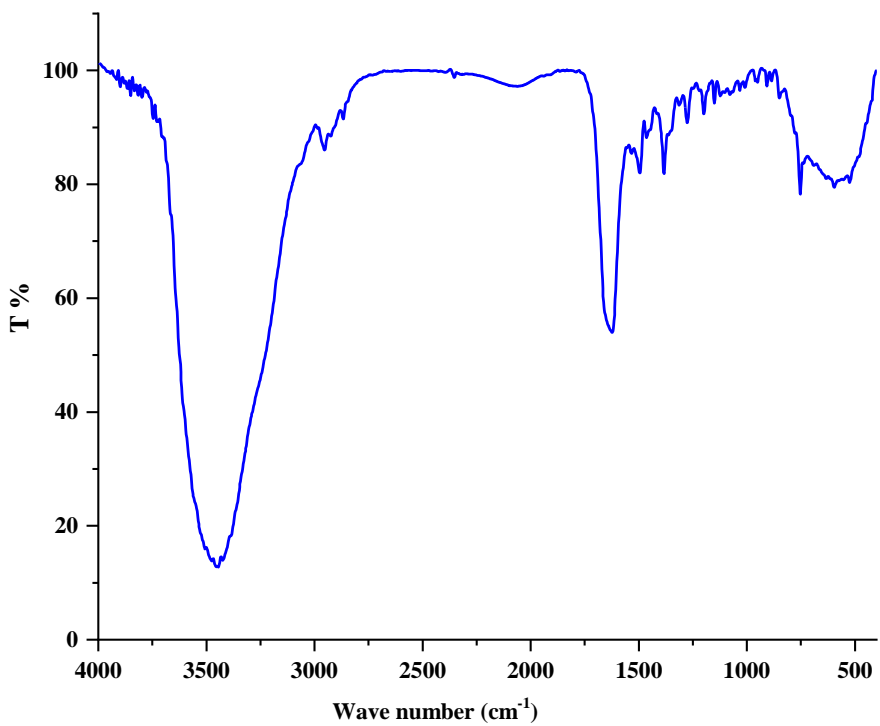


**Figure S5:** FTIR spectrum of  $[\text{Cu}(\text{L})(\text{H}_2\text{O})]\text{Cl}\cdot 2\text{H}_2\text{O}$  complex.

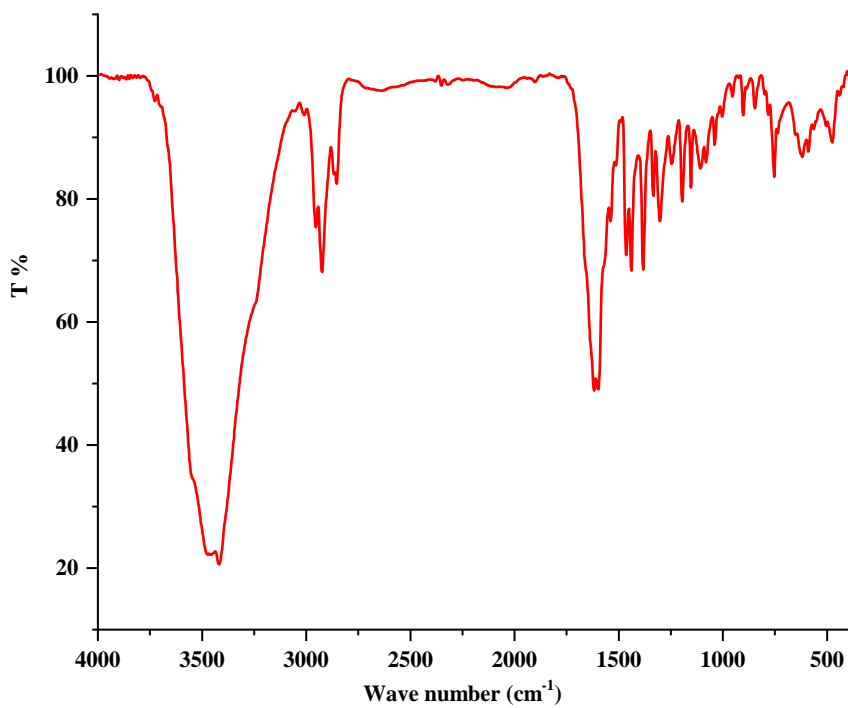


**Figure S6:** FTIR spectrum of  $[\text{Ni}(\text{L})_2]$  complex.

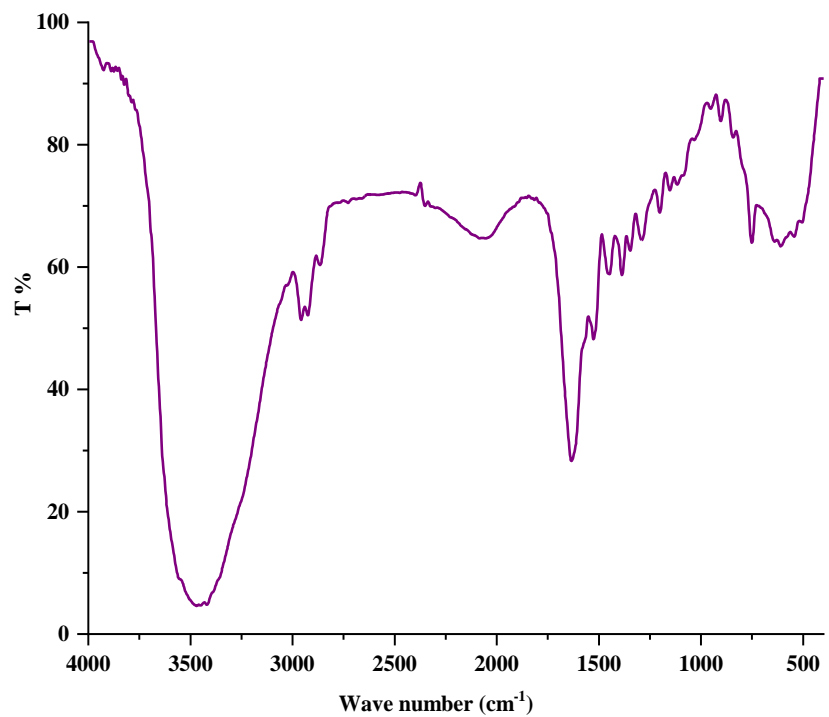


**Figure S7:** FTIR spectrum of  $[\text{Co}(\text{L})_2]\text{H}_2\text{O}$  complex.

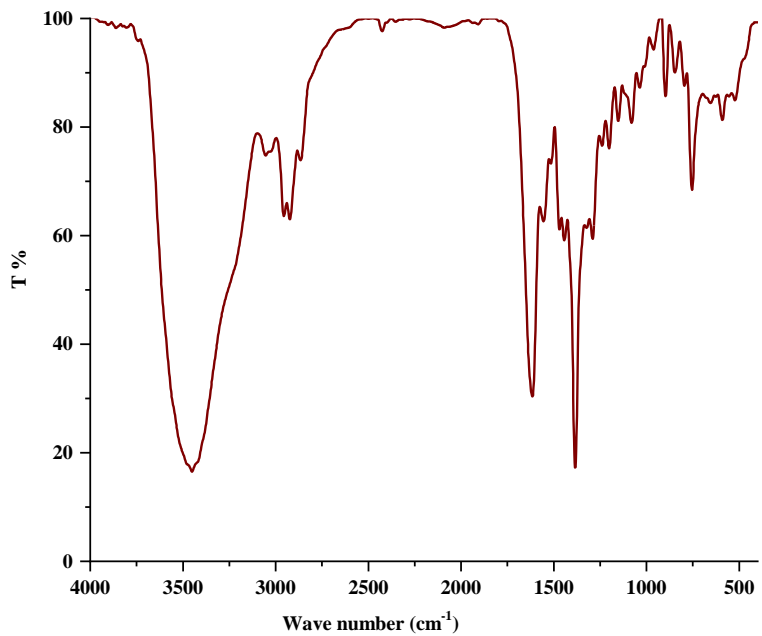


**Figure S8:** FTIR spectrum of  $[\text{Gd}(\text{L})_2(\text{H}_2\text{O})_2](\text{NO}_3)_3 \cdot 3\text{H}_2\text{O}$  complex.

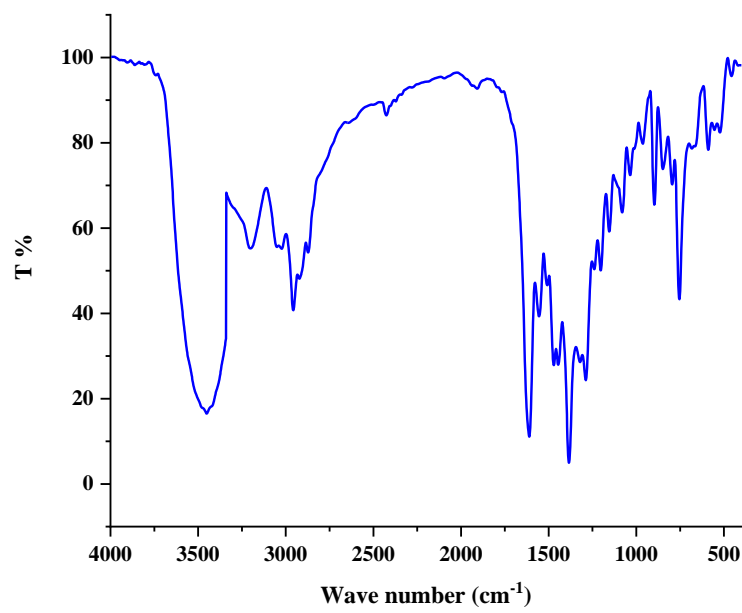


**Figure S9:** FTIR spectrum of  $[\text{Sm}(\text{L})_2(\text{H}_2\text{O})_2](\text{NO}_3)_2 \cdot 2\text{H}_2\text{O}$  complex.

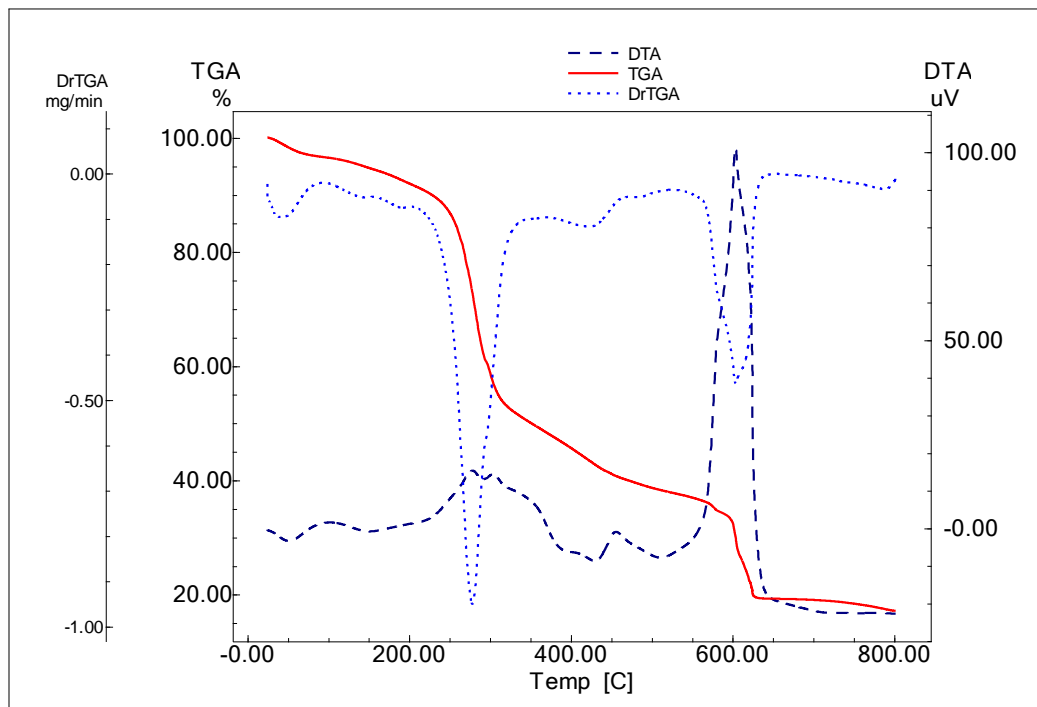


**Figure S10:** TGA/TG and DTA curves of  $[\text{Cu}(\text{L})(\text{H}_2\text{O})]\text{Cl} \cdot \text{H}_2\text{O}$  complex.

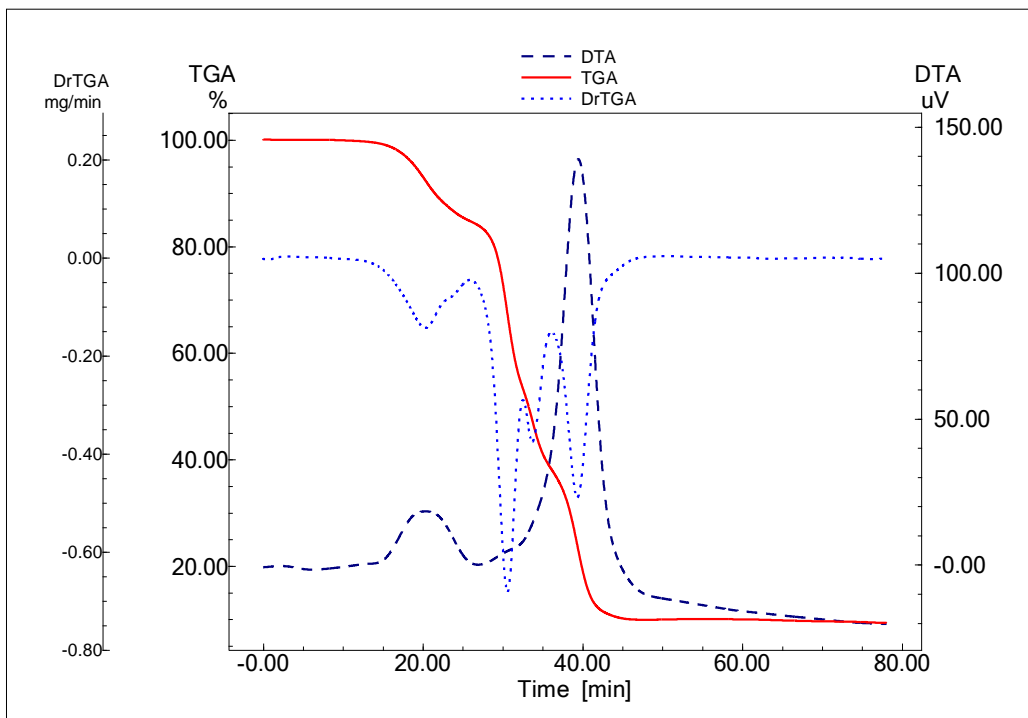


**Figure S11:** TGA/TG and DTA curves of  $[\text{Ni}(\text{L})_2]$  complex.

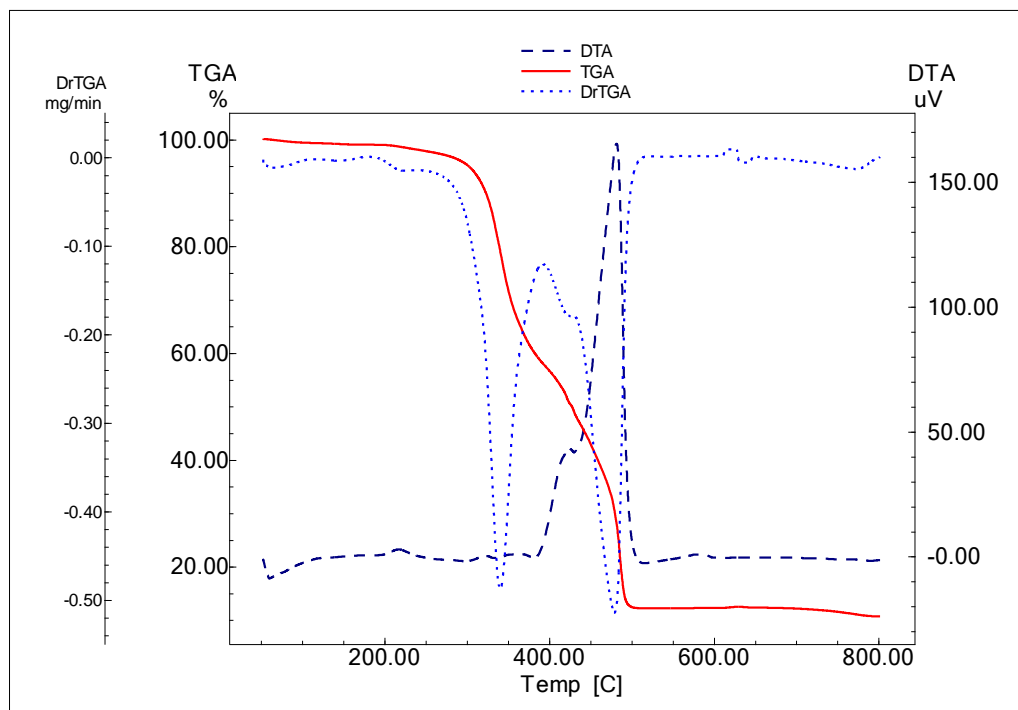


**Figure S12:** TGA/TG and DTA curves of  $[\text{Co}(\text{L})_2] \cdot \frac{1}{2}\text{H}_2\text{O}$  complex.

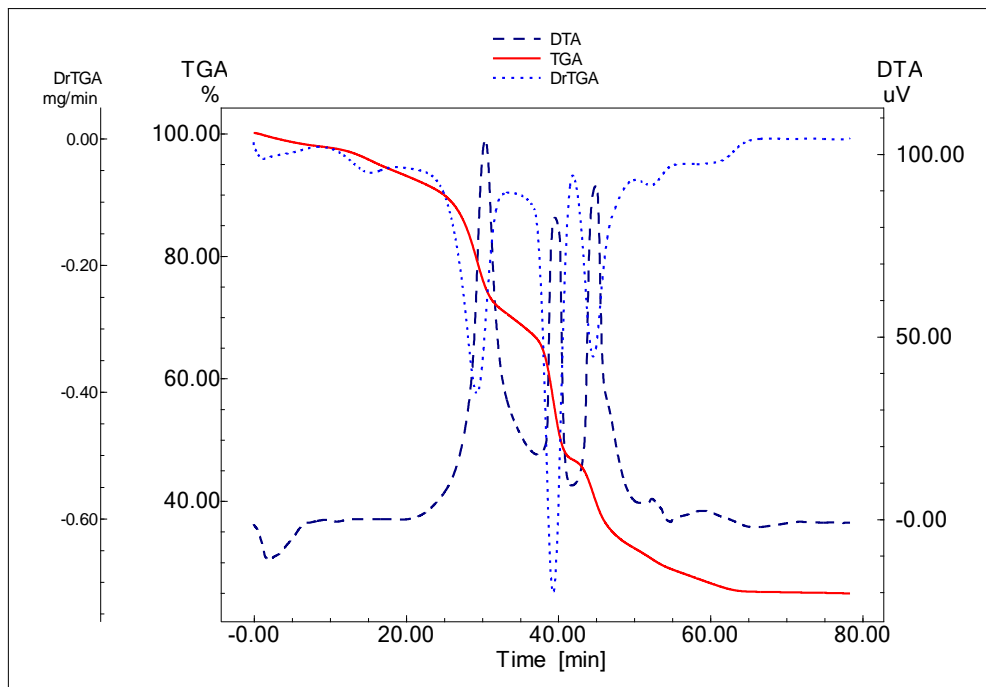


**Figure S13:** TGA/TG and DTA curves of  $[\text{Sm}(\text{L1})_2(\text{H}_2\text{O})_2](\text{NO}_3)_2 \cdot 2\text{H}_2\text{O}$  complex.

**Table S2:** DTA of Complexes derived from HL Schiff base.

<i>Compound</i>	<i>Temp. range °C</i>	<i>DTA peak temp °C</i>	<i>Peak type</i>	<i>ΔH (KJ/g)</i>	<i>Process</i>
	28-156	55	Endo	0.058	Dehydration+ Coordination sphere
$[\text{Cu}(\text{L})(\text{H}_2\text{O})]\text{Cl} \cdot \text{H}_2\text{O}$	160-514	278	Exo	-0.997	ligand degradation + Coordination sphere
	520-800	603	Exo	-2.24	Final degradation
$[\text{Ni}(\text{L})_2]$	119-300	235	Exo	-1.21	Ligand degradation
	311-786	449	Exo	-6.17	End degradation
	55-150	60	Endo	0.311	Dehydration
$[\text{Co}(\text{L})_2] \cdot 1/2\text{H}_2\text{O}$	156-278	218	Exo	-0.109	ligand degradation
	435-495	481	Exo	-7.9	Final degradation
	24-210	116	Endo	0.231	Dehydration

	307-	344, 412	Exo	-3.48	Coordination sphere+ Partial Ligand degradation
[Gd(L) <sub>2</sub> (H <sub>2</sub> O) <sub>2</sub> (NO <sub>3</sub> )]( NO <sub>3</sub> ) <sub>2</sub> · 3/2H <sub>2</sub> O	436-	509	Exo	-0.698	Ligand degradation
	569-	627	Exo	-1.01	Final degradation
	65-182	128	Endo	0.099	Dehydration + Coordination sphere
[Sm(L) <sub>2</sub> (H <sub>2</sub> O) <sub>2</sub> (NO <sub>3</sub> )] (NO <sub>3</sub> ) <sub>2</sub> ·2H <sub>2</sub> O	320- 350	345	Exo	-2.21	Coordination sphere+ Ligand degradation
	440- 469	446	Exo	-0.545	Ligand degradation
	474- 486	492,554	Exo	-1.14	Final degradation

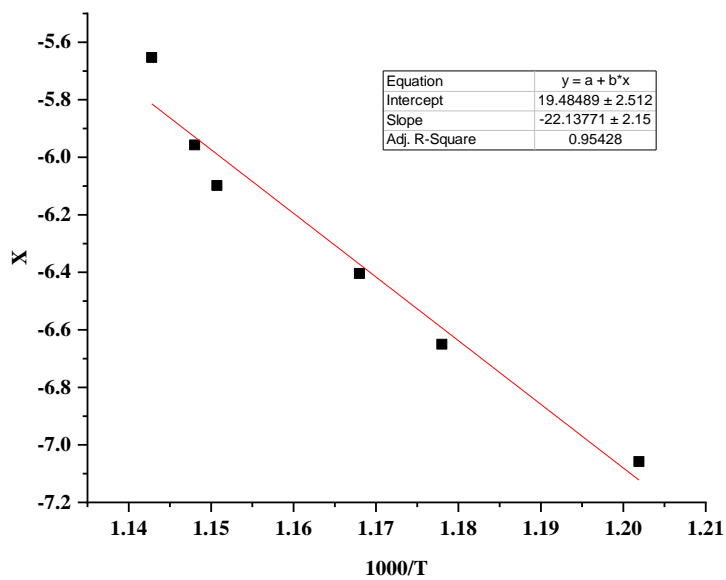
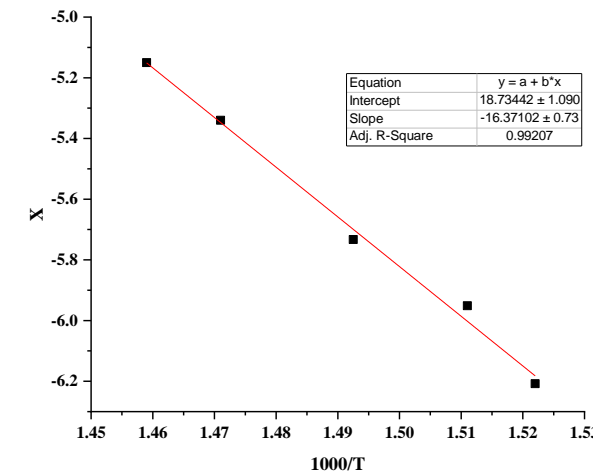
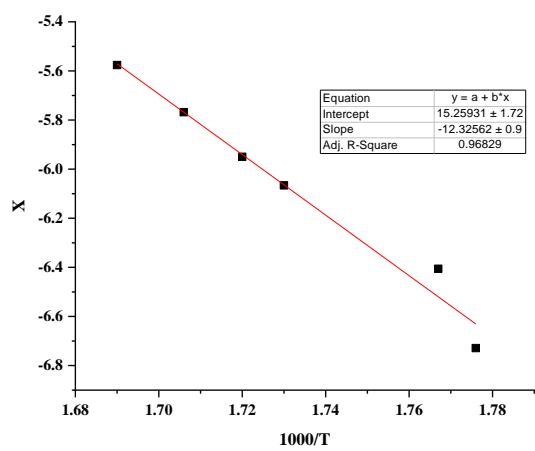
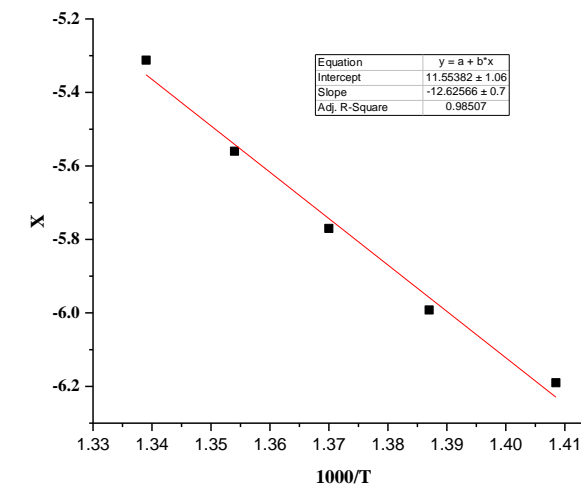
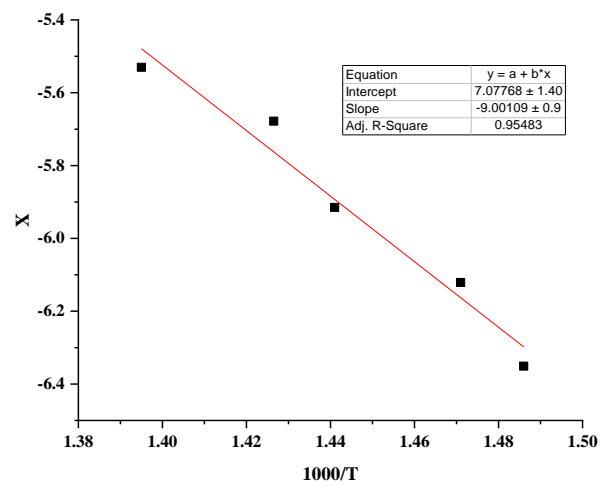


Figure S14: The fit-linear curve of the liberation of coordinate water step of **Cu-L1** complex.



**Table S3:** The electronic spectra and magnetic features of the **HL** ligand and its complexes.

Compound	Peak		$\epsilon^*$ ( $M^{-1}cm^{-1}$ ) $\times 10^4$	Assignment	10Dq			Postulated Structure
	nm	cm <sup>-1</sup>			cm <sup>-1</sup>	kJ/mol	$\mu_{eff}$ ( $\mu_B$ )	
<b>HL</b>	280	35714	5.57	$\pi \rightarrow \pi^*$	---	---	---	---
	290	34482	5.12		---	---	---	---
	322	31055	2.94	$n \rightarrow \pi^*$				
<b>L-Cu</b>	292	34246	2.27	$\pi \rightarrow \pi^*$	16556	201	1.49	Square planar
	363	27548	2.7	$n \rightarrow \pi^*$				
	404	24752	2.78	CT				
<b>L-Ni</b>	451	22172	11.86		24875	302	3.24	Distorted octahedral
	600	16556	0.05	d-d				
	317	31545	13.72	$n \rightarrow \pi^*$				
<b>L-Co</b>	400	25188	11.88	CT	19762	240	5.00	Octahedral
	628	24875	9.25	$^3A_{2g} \rightarrow ^1E_g$				
	290	34482	4.43	$\pi \rightarrow \pi^*$				
<b>L-Gd</b>	400	25000	4.58	$n \rightarrow \pi^*$	---	---	8.97	Bicapped trigonal prismatic / Square antiprismatic
	407	24570	4.56	$n \rightarrow \pi^*$				
	450	22222	3.13	CT				
<b>L-Sm</b>	506	19762	15.87	$^4T1g(F) \rightarrow ^4T2g(P)$				
	291	34364	3.21	$\pi \rightarrow \pi^*$				
	402	24875	3.25	$n \rightarrow \pi^*$				
<b>L-Ni</b>	452	22123	4.018	CT				
	504	19841	2.99					
	239	41841	16.32	$\pi \rightarrow \pi^*$				

\*  $\epsilon$ = Absorptivity,  $10^{-5}$  M in DMSO,  $M^{-1}cm^{-1}$ .

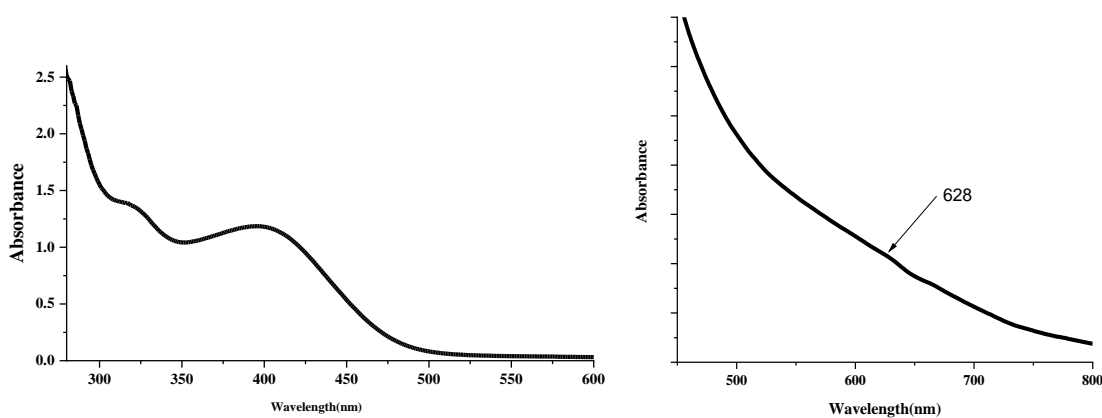


**Figure S19:** UV-Vis. spectrum of L1-Ni.

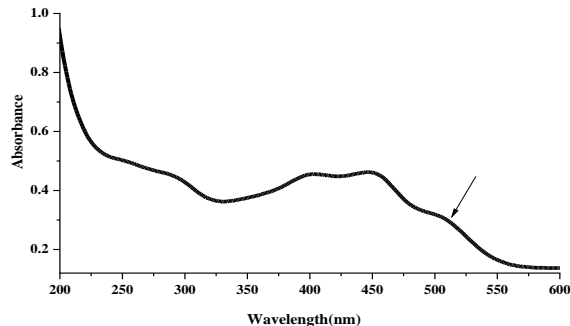


**Figure S20:** UV-Vis. spectrum of L1-Co.

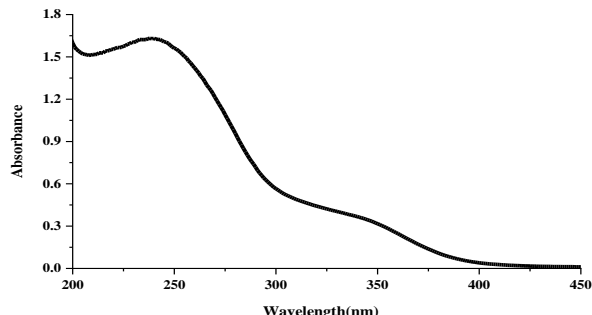


**Figure S21:** UV-Vis. spectrum of L1-Sm.

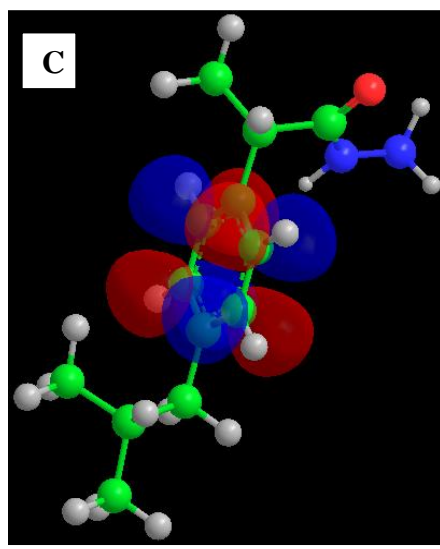
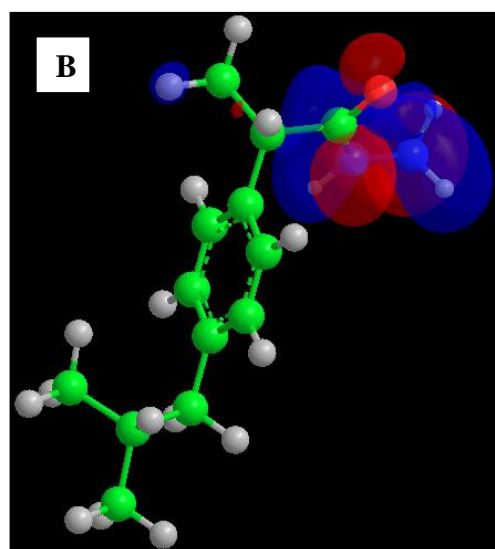
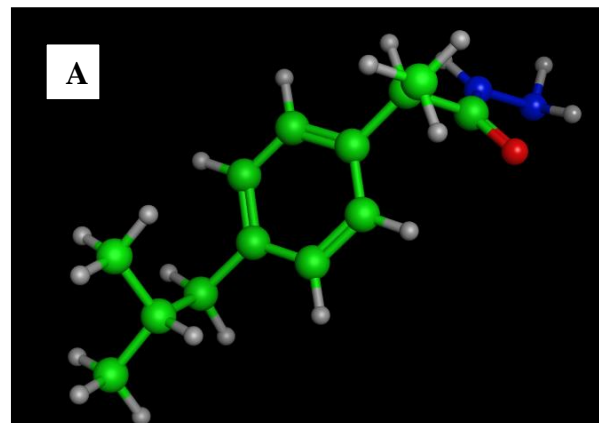


**Figure S22:** The DFT simulation for the Hydrazide Ibuprofen. (A) 3D view, (B) HOMO and (C) LUMO.

**Table S4:** The data from DFT calculations and the properties of synthesized compounds.

COMPOUND	IBUPROFEN	HI	HL	
FORMULA	C <sub>13</sub> H <sub>18</sub> O <sub>2</sub>	C <sub>13</sub> H <sub>20</sub> N <sub>2</sub> O	C <sub>20</sub> H <sub>24</sub> N <sub>2</sub> O <sub>2</sub>	
ATOMS	33	36	<b>48</b>	
ORBITALS	78	84	<b>120</b>	
ELECTRONS	82	88	<b>126</b>	
SCF ENERGY	-93.85 au	-98.24 au	<b>-144.94 AU</b>	
DIPOLE	1.94 d	3.37 d	<b>6.20 D</b>	
E <sub>LUMO</sub>	0.007	0.0036	<b>-0.012</b>	
E <sub>HOMO</sub>	-0.349	-0.351	<b>-0.325</b>	
E <sub>LUMO-HOMO</sub>	127.81 nm	128.56 nm	<b>145.36 NM</b>	
I (I.E)	0.348 au	0.351 au	<b>0.325 AU</b>	
ELECTRON AFFINITY (A)	-0.007 au	-0.004 au	<b>0.012 AU</b>	
ABSOLUTE ELECTRONEGATIVITY(X)	0.138	0.174	<b>0.168</b>	
ABSOLUTE HARDNESS ( )	0.211	0.177	<b>0.157</b>	
ABSOLUTE SOFTNESS ( )	4.739	5.640	<b>6.382</b>	
GLOBAL SOFTNESS (S)	2.370	2.820	<b>3.191</b>	
GLOBAL ELECTROPHILICITY ( )	0.045	0.085	<b>0.090</b>	
CHEMICAL POTENTIAL (PI)	-0.138	-0.174	<b>-0.168</b>	
ADDITIONAL ELECTRONEGATIVITY ( NMAX)	0.654	0.980	<b>1.073</b>	
TOXIC.	No	Yes	<b>NO</b>	
RSYNTH (%)	66.67	75	<b>79.17</b>	
WEIGHT (G/MOL)	206.28	220.32	<b>324.42</b>	
	37.30	55.12	<b>61.69</b>	
TPSA	Hd 1	Ha 2	Hd 2	HA 3
LOG P		3.07	1.98	<b>3.84</b>
LOG S		<b>-3.64</b>	<b>-3.90</b>	<b>-5.46</b>

\* SCF energy: self-consistent field, I: Ionization potential, Rsynth (%): Resynthesized %, TPSA: topological polar surface area, HD: Hydrogen donor, HA: Hydrogen acceptor, Log p: lipophilicity parameter and Log S: water solubility parameter.

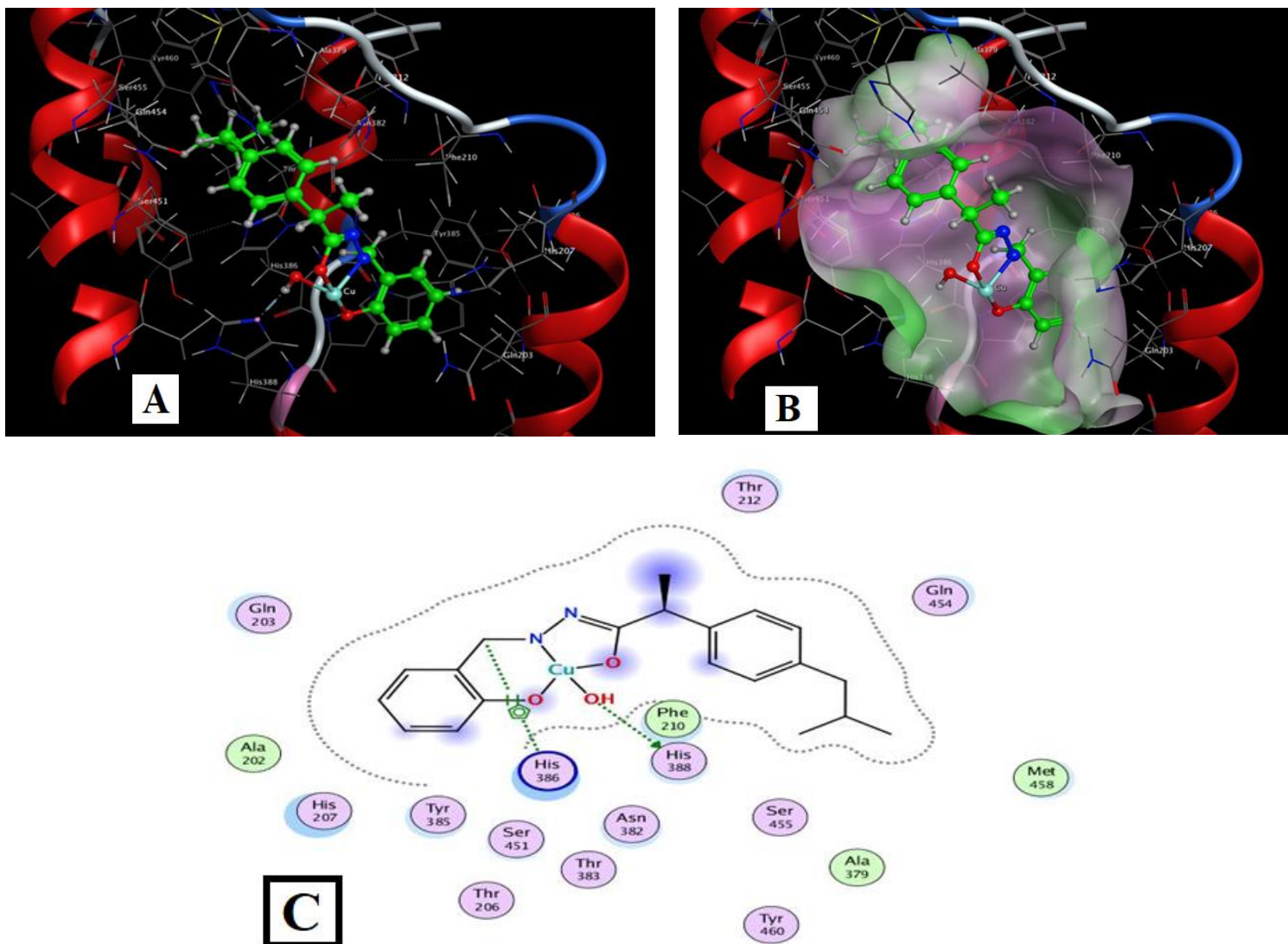


**Figure S23:** Docking model of the interaction of Cu-L1 with Cox2 [PDB code: 5IKT] bonding sites:

(A) 3D interaction diagram (B) The surface properties [Hydrophilic sites (violet color), neutral sites (white color) and lipophilic sites (green color)]. (C) 2D interaction diagram

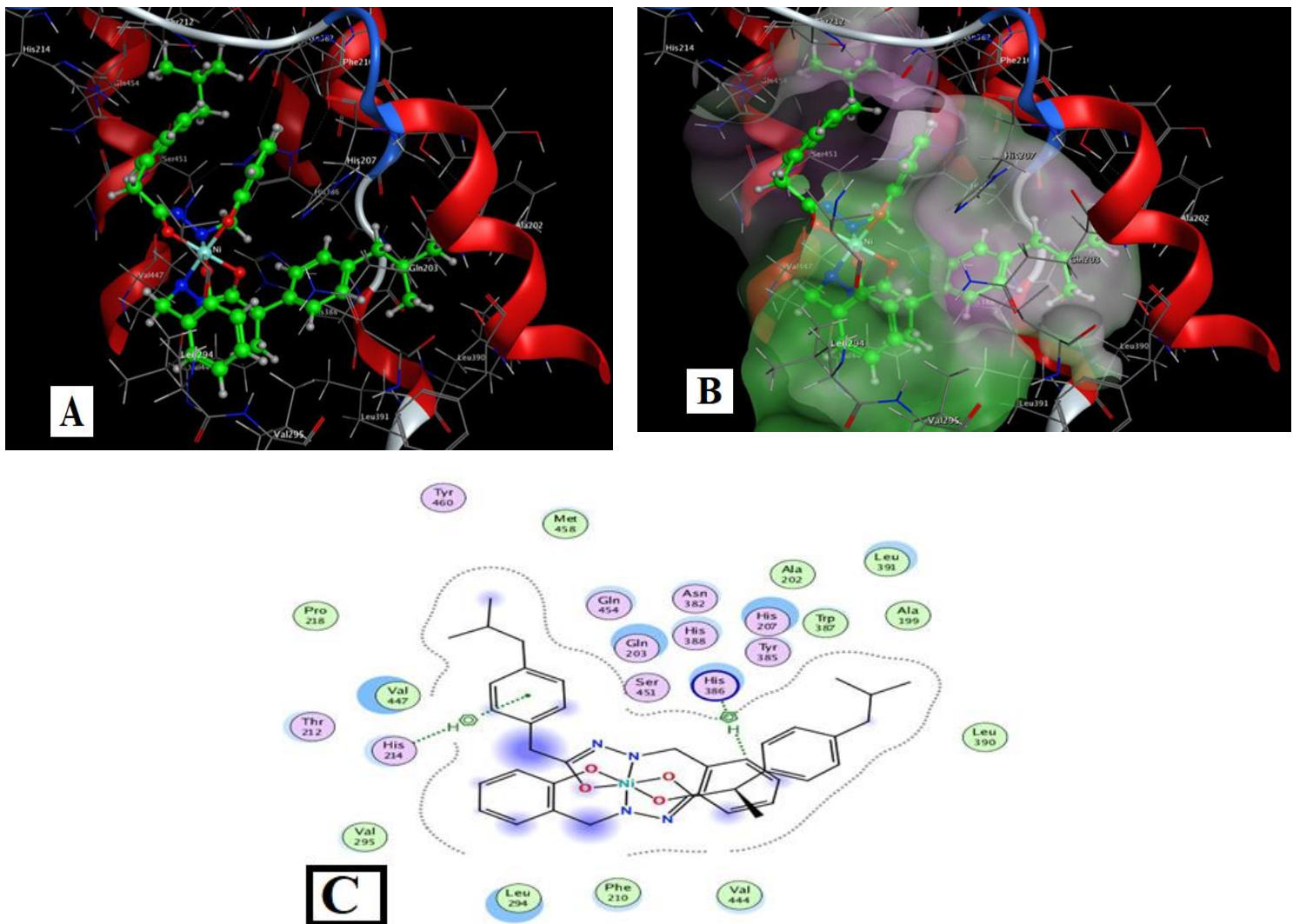


**Figure S24:** Docking model of the interaction of Ni-L1 with *Cox2* [PDB code: 5IKT] bonding sites:

(A) 3D interaction diagram (B) The surface properties [Hydrophilic sites (violet color), neutral sites (white color) and lipophilic sites (green color)]. (C) 2D interaction diagram

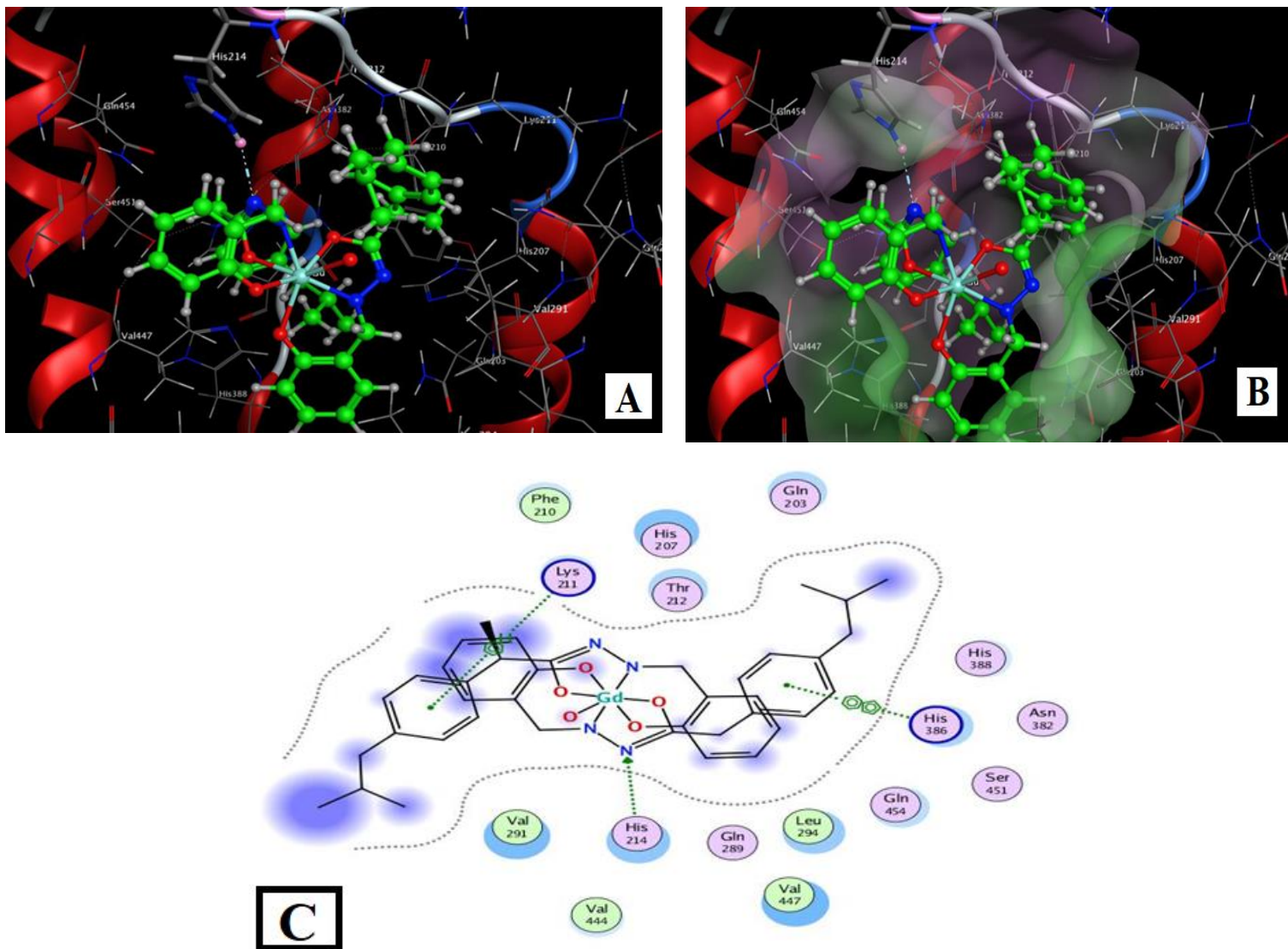


**Figure S25:** Docking model of the interaction of **Gd-L1** with **Cox2** [PDB code: 5IKT] bonding sites:

(A) 3D interaction diagram (B) The surface properties [Hydrophilic sites (violet color), neutral sites (white color) and lipophilic sites (green color)]. (C) 2D interaction diagram

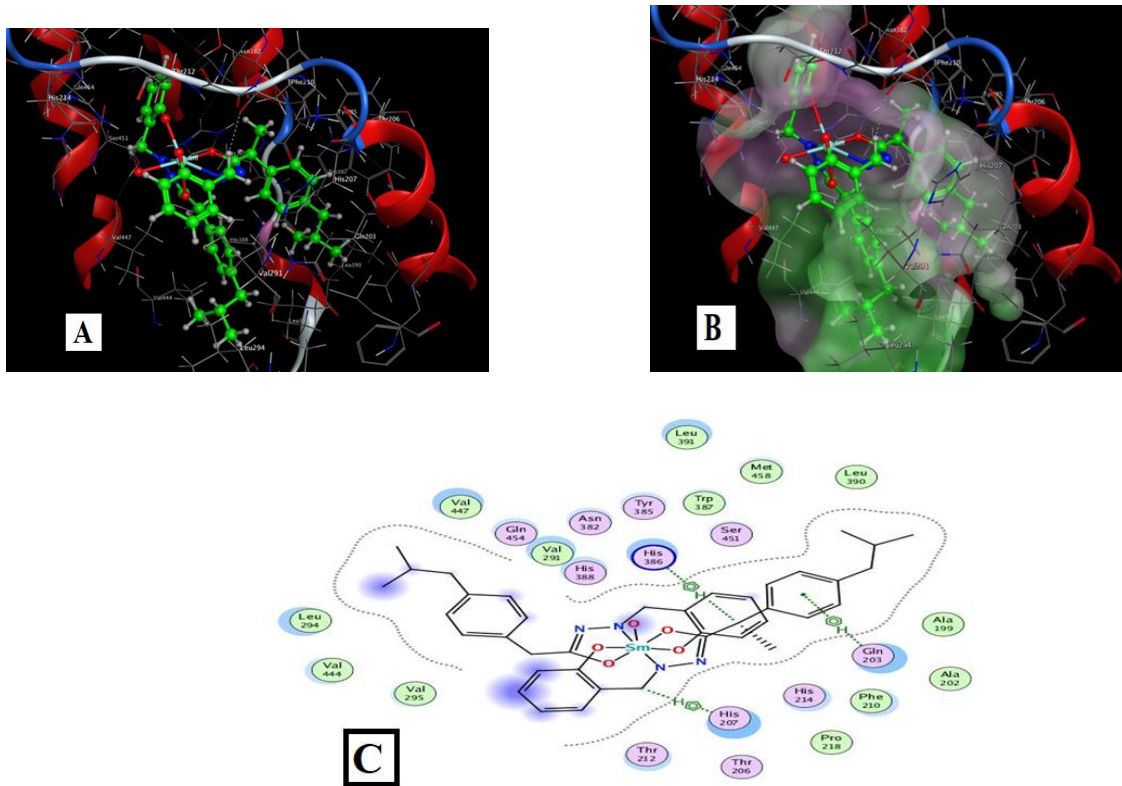


**Figure S26:** Docking model of the interaction of **Sm-L1** with **Cox2** [PDB code: 5IKT] bonding sites:  
 (A) 3D interaction diagram (B) The surface properties [Hydrophilic sites (violet color), neutral sites (white color) and lipophilic sites (green color)]. (C) 2D interaction diagram

**Table S5:** In vitro COX-1 and COX-2 inhibition of the synthesized derivatives.

Compound	COX-2 $IC_{50}$ ( $\mu M$ ) <sup>a</sup>
<b>Hydrazide</b>	4.3
<b>Schiff base (L)</b>	4.9
<b>Cu-L</b>	5.6
<b>Ni-L</b>	3.7
<b>Co-L</b>	1.7
<b>Gd-L</b>	2.3
<b>Sm-L</b>	2.9
<b>Ibuprofen</b>	31.4
<b>Indomethacin</b>	0.1
<b>Diclofenac sodium</b>	0.8